

Characterization and Evaluation of Electrical Properties of Corn Oil Biodiesel Blended with TiO₂ Nano Additives

Janaki Pakalapati^{†*} , Raviteja Surakasi ^{**} , Ramya Pakalapati ^{***} , K.Trinadh Babu ^{****} 

*+ Department of Electrical and Electronics Engineering, Lendi Institute of Engineering and Technology, Jonnada, Vizianagaram, Andhra Pradesh, India – 535005

** Department of Mechanical Engineering, Lendi Institute of Engineering and Technology, Jonnada, Vizianagaram, Andhra Pradesh, India - 535005

*** Department of Mechanical Engineering, Anil Neerukonda Institute of Technology and Sciences (ANITS), Sangivalasa, Bheemunipatnam, Visakhapatnam, Andhra Pradesh, India – 531162

**** Department of Electrical and Electronics Engineering, Anil Neerukonda Institute of Technology and Sciences (ANITS), Sangivalasa, Bheemunipatnam, Visakhapatnam, Andhra Pradesh, India - 531162

(ravitejasurakasi@gmail.com, janaki.pakalapati@gmail.com, ramyapakalapati87@gmail.com, ramyapakalapati87@gmail.com)

† Corresponding Author; Raviteja Surakasi, Department of Mechanical engineering, Lendi institute of engineering and technology, Jonnada, Vizianagaram, Andhrapradesh, India - 535005, Tel: +91 8142515393, ravitejasurakasi@gmail.com

Received: 21.04.2023 Accepted:24.05.2023

Abstract- The fundamental objective of this research is to assess the electrical properties of nanopowder corn oil biodiesel. Initially, corn oil biodiesel is prepared by transesterification process and mixed with TiO₂ nanopowder in different of 0.025%, 0.05%, 0.075%, and 0.1%. TiO₂ nanofluids are examined using SEM and TEM. The morphology of TiO₂ nanoparticles was analysed using SEM. It appeared that the average size of the TiO₂ particles created in this way was 27 nm. The electrical properties of prepared biodiesel blends are evaluated, such as their breakdown voltage, permittivity, resistivity, and dissipation factor. With the increase in the diameter, there is an increase in the value of resistivity with the dispersion of TiO₂ nano powder whereas breakdown voltage, permittivity, and electrical conductivity have been decreased with the increase in the diameter. Overall with the dispersion of TiO₂ nano powder the electrical properties have been enhanced.

Keywords: Corn Oil, Electrical conductivity, breakdown voltage, permittivity, resistivity

1. Introduction

Corn oil biodiesel is a renewable fuel that is gaining popularity as an alternative to traditional fossil fuels in recent years due to its environmental benefits [1-6]. However, biodiesel has some drawbacks such as poor cold flow properties, low oxidative stability, and low electrical conductivity [7-9]. The low electrical conductivity of biodiesel can affect its performance in fuel injection and ignition systems, leading to incomplete combustion and reduced engine performance [10-12]. To address this limitation, researchers have investigated the use of nanoparticles as additives to improve the electrical properties

of biodiesel. TiO₂ nanopowders are commonly used as conductive additives due to their high electrical conductivity and high surface area [13-18]. These nanoparticles can increase the electrical conductivity of biodiesel by acting as conductive pathways for electrons. They can also improve the dielectric strength of the fuel, which is important for preventing ignition and maintaining the safety of the fuel. In this research paper [14]. The aim is to investigate the effect of TiO₂ nanopowder on the electrical properties of corn oil biodiesel. It will examine the electrical conductivity and dielectric strength of the fuel with and without nanoparticle additives [15]. It will also investigate the effect of nanoparticle concentration and size on the electrical

properties of the fuel. This research is of great interest to the biodiesel industry and researchers working on developing more efficient and sustainable energy systems. The findings of this study could lead to the development of new and improved biodiesel fuels with better electrical properties, which could pave the way for their wider adoption in various industries.

2. Preparation of Biodiesel Samples



Fig.1. Biodiesel preparation process

The Corn oil of 1200ml is heated up to 40°C on a Magnetic Stirrer or Mixer. Then, combine 3.5 grams of sodium hydroxide (KOH) pellets with 125 mm of methanol. Turn down the heat as soon as the oil reaches a temperature of 56°C to 58°C. Let the oil for an hour settle. Let the oil settle down with its fatty acids and glycerol [16]. Now separate the glycerol from the oil with the help of a separating funnel. Later separation rinses the oil with distilled water or Hot water thoroughly. And reheat the obtained oil one more time up to 90°C on Magnetic Stirrer to evaporate the water bubbles which may be present in it. Collect the oil into container bottles and process it to blending [17]. Figure 1. shows the biodiesel preparation process

2.1 Blending of Fuel

The first step in blending biodiesel is to determine the desired blend ratio. This is usually expressed as a percentage of biodiesel to petroleum diesel, such as B5 (5% biodiesel, 95% petroleum diesel) or B20 (20% biodiesel which is prepared using corn oil, 80% petroleum diesel). After preparing Biodiesel with desired blend ratio, then it is mixed in the proportions of 0.025%, 0.05%, 0.075%, and 0.1%. of TiO₂ respectively using Ultrasonicator equipment [18]. The prepared biodiesel blended nano additives are used for the analysis of breakdown voltage, dielectric constant, dissipation factor, and resistivity.

2.2 Properties of Titanium dioxide (TiO₂)

Titanium dioxide (TiO₂) is a mineral found in nature and has several practical uses in industry. Water and also most organic solvents are unable to dissolve this white, odourless powder [19]. TiO₂ is a versatile material thanks to its high refractive index, low toxicity, and resilience to UV light, among other physical and chemical features. TiO₂ is commonly used in the production of pigments for paints, plastics, and ceramics due to its opacity and ability to reflect light. It is also used as a photocatalyst for air and water purification, as well as in the production of solar cells and other electronic devices. TiO₂'s potential in biological applications including drug transport and cancer therapy has been the subject of many studies. TiO₂ nanoparticles' rising popularity may be attributed to a number of factors, including their high surface area and their reactivity [20]. Yet, their potential risks to ecosystems as well as human health haven't been thoroughly evaluated. Figure 2. shows the TiO₂ nano powder.



Fig.2. TiO₂ Nanopowder

3. Methodology and Characterization

Nanoparticles' attributes were studied in depth. From 10 to 80 degrees Celsius, an X-ray diffractometer having 40 kV/15mA radiation examined TiO₂ nanoparticle structural characteristics. Shimadzu 2700 UV-visible spectrophotometers assessed titanium dioxide nanoparticle absorption. High-resolution scanning electron microscopy (SEM Carl ZEISS) and energy-dispersive X-ray spectroscopy were utilised to investigate generated TiO₂ nanoparticles, followed by chemical analysis using PerkinElmer FT-IR (400-4000cm⁻¹). Transmission electron microscopy examined nanoparticle surface texture (Titan).

3.1 SEM and TEM Analysis of TiO₂ Nanoparticles

By scanning an electron beam over a sample, scanning electron microscopy produces a magnified picture of the sample (SEM). Microanalysis, including failed examination of solid inorganic compounds, may be performed using scanning electron microscopy (SEM) or scanning electron analysis (SEM). Indicators of electron interaction are generated by the scanning electron microscope, which uses kinetic energy as its working principle [21]. The SEM, and TEM images containing TiO₂ nanoparticles are shown in Figure 3. and Figure 4. respectively. Secondary electrons, such as backscattered electrons as well as diffracted backscattered electrons, are needed to see crystalline

elements as well as photons. The average size of the synthesised TiO₂ particles was estimated to be 27 nm.

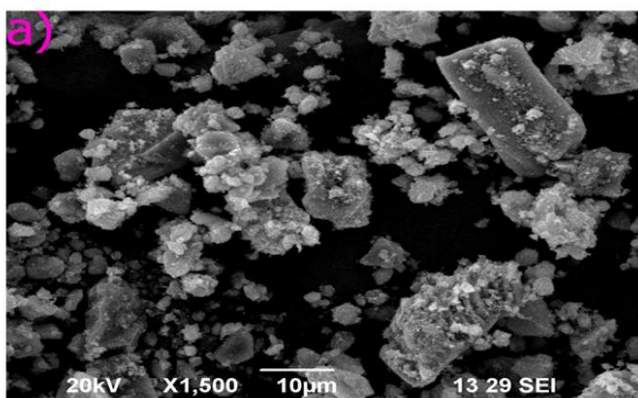


Fig. 3. SEM images of TiO₂ NPs.

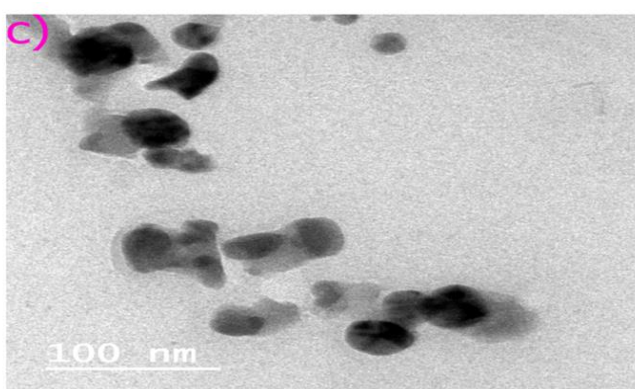


Fig. 4. TEM micrograph of TiO₂ NPs.

3.2 Breakdown Voltage

Breakdown voltage refers to the minimum voltage required to cause a material, such as an insulator or a semiconductor, to conduct electricity. In other words, it is the voltage at which the material's electrical resistance decreases significantly, and it becomes able to conduct electrical current. Breakdown voltage can occur in several ways, depending on the material and the conditions [22]. Some common types of breakdown voltage include Zener breakdown: This occurs in heavily doped p-n junctions in diodes. When the reverse-bias voltage across the junction reaches a certain threshold, called the Zener voltage, the junction breaks down and conducts current in the reverse direction. Avalanche breakdown: This occurs in materials such as semiconductors when a high electric field causes free electrons to gain enough kinetic energy to knock other electrons free, creating a cascade effect that leads to a large current. Dielectric breakdown [23]. This occurs in insulating materials when the electric field becomes strong enough to ionize atoms or molecules in the material, creating a conductive path. Several electrical applications rely on a material's breakdown voltage, which may be altered by environmental conditions such as temperature and humidity as well as by the presence of contaminants or flaws.

3.3 Dielectric Constant

The dielectric constant (or relative permittivity) quantifies a material's capacity to absorb and release electric energy in a given electric field. The electric flux density is a ratio between the electric flux density in the material and the electric flux density in a vacuum, and it is a dimensionless quantity. When an electric field is applied to a material, the amount of polarization it undergoes is measured by a property known as the dielectric constant. Materials with a high dielectric constant are able to store more electrical power in a magnetic field than those with a low dielectric constant [24]. The dielectric constant is an important property for many electrical applications. For example, it is used in the design of capacitors, which are electrical components that store energy in an electric field. Materials with a high dielectric constant are often used in capacitors because they can store more energy for a given size of the capacitor. The dielectric constant can also be affected by factors such as temperature, pressure, and frequency. For example, the dielectric constant of a material may decrease at high temperatures, which can affect the performance of electrical components made from that material.

3.4 Dissipation Factor

In an electric field, the dissipation factor (or loss tangent) quantifies the rate at which energy is lost by a substance. The term refers to the proportion of a material's power loss relative to its power transmission [25]. Whenever an electrical field is applied toward a material, the quantity of energy dissipated as heat is measured by the dissipation factor. When the dissipation factor is high, the material gives out a lot of heat, whereas when it's low, the material keeps releasing more electrical energy in the form of heat. The dissipation factor is an important characteristic of materials used in electrical applications, as it can affect the performance and efficiency of electrical components. For example, in a capacitor, a high dissipation factor can cause the capacitor to generate heat, which can reduce its performance and lifespan [26]. The dissipation factor can be affected by various factors such as temperature, frequency, and the composition of the material. For example, the dissipation factor of a material may increase at higher frequencies, which can affect the performance of electrical components made from that material.

3.5 Resistivity

A material's resistivity may be seen as a measurement of the intrinsic resistance that it presents to the passage of electrical current. The electrical conductivity of a material is a basic feature that may be described as the ratio of said electrical field that is imposed on it to the electrical current density that is produced by the material. To put it another way, resistivity is a measurement of how straightforward or challenging it is for an electrical current to travel through a substance. Materials that have a high resistivity also have a high degree of electrical resistance but aren't excellent conductors of electricity [27]. On the other hand, materials that have a low resistivity also have a low degree of electrical resistance and thus are good conductors of electricity. There are a number of variables that may influence the resistivity of

a material. Some of these factors include temperature, pressure, the existence of impurities or flaws in the material, and the presence of both. As an example, the resistivity of the vast majority of metals rises with increasing temperature, but the resistivity of semiconductors falls with increasing temperature [28]. Because of its role in determining a material's electrical conductivity and its overall efficiency, resistivity is an essential attribute in a wide variety of electrical applications. Electrical components like cables and circuit boards rely heavily on calculations of the resistance of a material with a certain cross-section and thickness. In the International System of Units, the ohm-meter (m^*) is the symbol used to indicate resistivity (SI). Conductivity, which is the inverse of resistivity, is another significant characteristic in electrical applications. It is termed the inverse of resistivity.

4. Experimental Setup



Fig. 5. Transformer oil apparatus

The electrodes are subjected to an ac voltage whose frequency ranges from 40 to 60 hertz, with the voltage gradually increased from zero to the point where the breakdown occurs at a rate of 2 kilovolts per second [29]. The procedure must be repeated six times with the same cell filling. The initial application of voltage after each breakdown occurs as quickly as feasible following cell filling, but no more than ten minutes after filling to ensure that almost no air bubbles exist in the oil. After gently swirling the oil between the electrodes with clean, dry glasses for a minute to remove any air bubbles which might have formed, the voltage is restored for further flue testing [30]. Figure 5. depicts the oil transformer arrangement.

5. Results and Discussion

5.1 Break Down Voltage

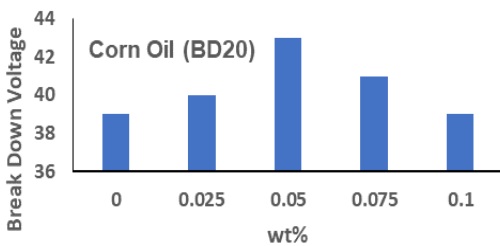


Fig. 6. Weight percent Vs breakdown voltage for TiO₂

Figure 6. shows the Graph drawn between the weight percentage of TiO₂ and Breakdown Voltage. It is evident that with the increase of TiO₂ to 0.05% the Breakdown Voltage increases. Further increase of TiO₂ from 0.05% to 0.1% gives declining results [31]. The minimum Breakdown Voltage is 39kV at 0% of TiO₂ (i.e., BD20).

5.2 Dielectric Constant

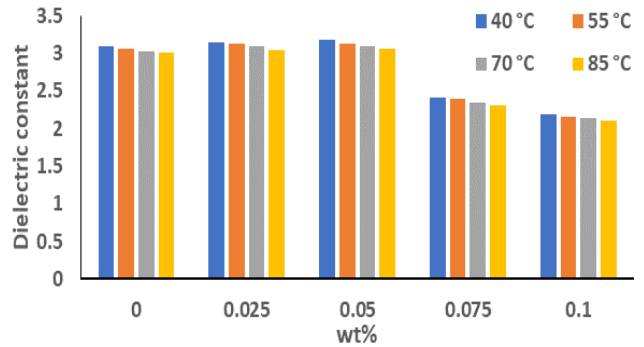


Fig. 7. Weight percent Vs dielectric constant for TiO₂

Figure 7. explains the graph drawn between the weight percentage of TiO₂ and the Dielectric Constant. It is understood that with an increase in weight percentage to 0.05% TiO₂ the Dielectric Constant increases [25]. Further increase of weight percent from 0.05 to 0.1 gives declining results. For Corn Oil (BD20) the minimum dielectric constant is 3 at 85°C. For Corn Oil with 0.025% TiO₂ (BD20+25ppm TiO₂) the minimum dielectric constant is 3.04 at 85°C. For Corn Oil with 0.05% TiO₂ (BD20+50ppmTiO₂), the minimum dielectric constant is 3.06 at 85°C. For Corn Oil with 0.075% TiO₂ (BD20+50ppm TiO₂) the minimum dielectric constant is 2.31 at 85°C. For Corn Oil with 0.1% TiO₂ (BD20+50ppm TiO₂) the minimum dielectric constant is 2.11 at 85°C [33]. It concludes that the minimum dielectric constant is 2.11 for Corn Oil with 100ppm of TiO₂ at 85°C.

5.3 Dissipation factor

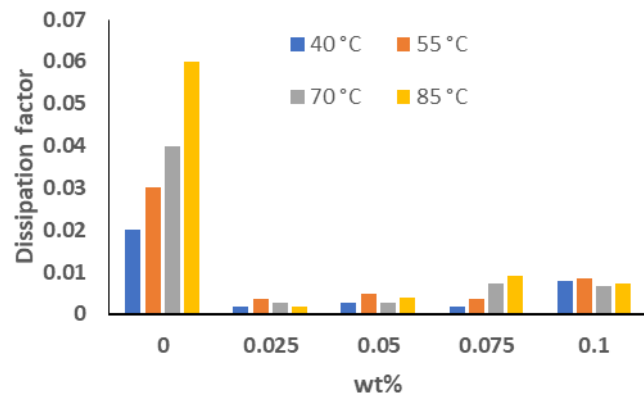


Fig. 8. Weight percent Vs dissipation factor for TiO₂

Figure 8. explains the graph drawn between the weight percentage of TiO₂ and the Dissipation factor. It is observed that the Dissipation factor increases with the increase of weight percent to 0.05% at 40°C and 55°C, 0.075% at 70°C and 85°C [28]. Further increase of weight percent gives declining results. For Corn Oil (BD20) the minimum

dissipation factor is 0.02 at 40°C. For Corn Oil with 0.025% TiO₂ (BD20+ 25ppm TiO₂), the minimum dissipation factor is 0.0017 at 85°C. For Corn Oil with 0.05% TiO₂ (BD20+ 50ppm TiO₂), the minimum dissipation factor is 0.0027 at 40°C. For Corn Oil with 0.075% TiO₂ (BD20+ 75ppm TiO₂), the minimum dissipation factor is 0.0018 at 40°C [18]. For Corn Oil with 0.1% TiO₂ (BD20+ 100ppm TiO₂), the minimum dissipation factor is 0.0068 at 70°C. It concludes that the minimum Dissipation factor is 0.0017 for Corn Oil with 0.025% of TiO₂ at 85°C.

5.4 Resistivity

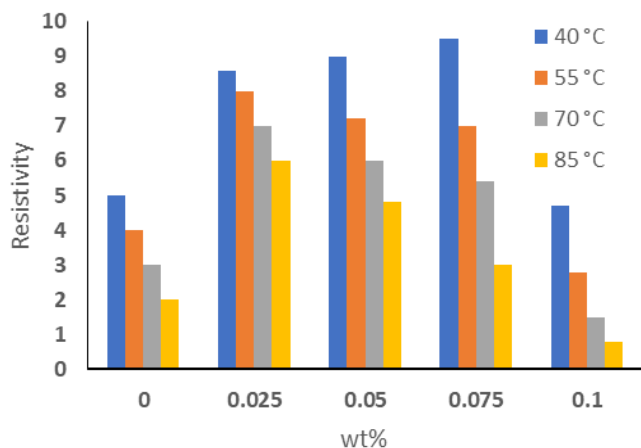


Fig. 9. Weight percent Vs resistivity for TiO₂

Figure 9. explains the graph drawn between the weight percentage of TiO₂ and Resistivity. It is observed that with the increase of weight percentage of TiO₂ to 0.025% and 0.075% of TiO₂ the Resistivity increases [23]. Further increase of TiO₂ gives declining results. For Corn Oil (BD20) the maximum resistivity is 5 Ω at 40°C. For Corn Oil with 0.025% TiO₂ (BD20+25ppm TiO₂), the maximum resistivity is 8.6 Ω at 40°C. For Corn Oil with 0.05% TiO₂ (BD20+50ppm TiO₂), the maximum resistivity is 9 Ω at 40°C. For Corn Oil with 0.075% TiO₂ (BD20+75ppm TiO₂), the maximum resistivity is 9.5 Ω at 40°C. For Corn Oil with 0.1% TiO₂ (BD20+100ppm TiO₂), the maximum resistivity is 4.7 Ω at 40°C. It concludes that the maximum resistivity is 9.5 Ω for Corn Oil with 0.075% of TiO₂ at 40°C.

6. Conclusions

The diameter of the nanoparticles was determined to be 27 nm using the Debye-Scherrer equation. SEM and TEM examinations confirmed the nanoparticles' claimed dimensions and spherical form. While comparing different weight percentages of nano additives for breakdown voltage, the minimum Breakdown Voltage is 39 kV for Corn Oil (BD20 (20% biodiesel which is prepared using corn oil, 80% petroleum diesel)). Upon comparing different weight percent of TiO₂ nano additives, the Minimum Dielectric Constant is 2.11 for Corn Oil with 0.1% TiO₂ at 85°C. When comparing different weight percent TiO₂ nano additives, the Minimum Dissipation factor is 0.0017 for Corn Oil with 0.025% of TiO₂ at 85°C. Upon comparing different weight percent TiO₂ nano additives, It concludes that the maximum resistivity is 9.5 Ω for Corn Oil with 0.075% of TiO₂ at 40°C.

Future Scope

Further experiments can be conducted using different edible and non-edible oils and prepare biodiesels from them and disperse them with different metallic and non-metallic nano additives to enhance their electrical properties.

Data Availability

The article contains all of the data needed to prove the study's claims.

Conflicts of Interest

All authors have stated that they have no competing interests related to this research.

References

- [1] G. Vaidya, P.P. Patil, A.S. Sener, N.S. Ramnath, B. Singh, R. Surakasi, S. Sripathi, and T.A. Atiso, "Chlorella protothecoides Algae Oil and Its Mixes with Lower and Higher Alcohols and Al₂O₃ Metal Nano additives for Reduction of Pollution in a CI Engine", *J. Nanomater.*, vol. 2022, pp.1- 6, 2022.
- [2] J. Arunprasad, A.N. Krishna, D. Radha, M. Singh, R. Surakasi, and T.D. Gidebo, "Nanometal-Based Magnesium Oxide Nanoparticle with *C. vulgaris* Algae Biodiesel in Diesel Engine", *J. Nanomater.*, vol. 2022, pp.1- 9, 2022.
- [3] R. Surakasi, M.K Khan, A.S. Sener, T. Choudhary, S. Bhattacharya, P. Singhal, B. Singh, and V.L. Chowdary, "Analysis of Environmental Emission Neat Diesel-Biodiesel–Algae Oil-Nanometal Additives in Compression Ignition Engines", *J. Nanomater.*, vol. 2022, pp.1-7, 2022.
- [4] R. Surakasi, S. Sripathi, S.P. Nadimpalli, S. Afzal, B. Singh, M. Tripathi, and R.A. Hafa, "Synthesis and Characterization of TiO₂-Water Nanofluids", *Adsorp. Sci. Technol.*, vol. 2022, pp.1-9, 2022.
- [5] R. Surakasi, K.C. Sekhar, E. Yanmaz, G. Yuvaraj, J. Venugopal, S. Srujana, and N. Begum, "Evaluation of Physic thermal Properties of Silicone Oil Dispersed with Multiwalled Carbon Nanotubes and Data Prediction Using ANN", *J. Nanomater.*, vol. 2021, pp.01-11, 2021.
- [6] M.E. Meibodi, M.V. Sefti, A. Rashidi, and H.S. Kalal, "The role of different parameters on the stability and thermal conductivity of carbon nanotube/water nanofluids," *Int. Commun. Heat Mass Transf.*, vol. 37, pp. 319–323, 2010.
- [7] K.C. Sekhar, R. Surakasi, I. Garip, S. Srujana, V.V. Prasanna Kumar, and N. Begum, "Evaluation of Physicothermal Properties of Solar Thermic Fluids Dispersed with Multiwalled Carbon Nanotubes and Prediction of Data Using Artificial Neural Networks", *J. Nanomater.*, vol. 2021, pp.1-13, 2021.
- [8] S. Karthikeyan, and T. Dharma Prabhakaran, "Emission analysis of *Botryococcus braunii* algal

- biofuel using Ni-Doped ZnO nano additives for IC engines,” *Energ. Source Part A*, vol.40, pp.1060–1067, 2018.
- [9] S. Karthikeyan, K. Kalaimurugan, A. Prathima, and D. Somasundaram, “Novel microemulsion fuel additive Ce–Ru–O catalysts with algae biofuel on diesel engine testing,” *Energ. Source Part A*, vol.40, pp.630–637, 2018.
- [10] S. Karthikeyan, K. Kalaimurugan, and A. Prathima, “Quality analysis studies on biodiesel production of neochloris oleoabundans algae,” *Energ. Sources Part A*, vol. 40, pp. 439–445, 2018.
- [11] S. Karthikeyan, A. Prathima, M. Periyasamy, and G. Mahendran, “Analysis of steel ST 75 using tribotester pin-on-disc,” *Elsev. Mater. Today Proceed.*, vol.33, pp.4285–4288, 2020.
- [12] S. Karthikeyan, A. Prathima, M. Periyasamy and G. Mahendran, “Assessment of the use of Codium Decorticaefum [Green seaweed] biodiesel and pyrolytic waste tires oil blends in CI engine, *Elsev. Mater. Today Proceed.*, vol.33, pp.4224– 4227, 2020.
- [13] S. Karthikeyan, A. Prathima, M. Periyasamy and G. Mahendran “Performance analysis of Al_2O_3 and $C_{18}H_{34}O_2$ with Kappaphycus Alvarezil-Brown algae biodiesel in CI engine,” *Elsev. Mater. Today Proceed.*, vol.33, pp.4180–4184, 2020.
- [14] S. Karthikeyan, A. Prathima, M. Periyasamy, and G. Mahendran, “Impact of using single injection strategies and of Kappaphycus Alvarezil algae biodiesel on a diesel engine with common injection ramp,” *Elsev. Mater. Today Proceed.*, vol.33, pp.4621–4625, 2020.
- [15] S. Karthikeyan, A. Prathima, M. Periyasamy, and G. Mahendran, “Emission assessment of Kappaphycus Alvarezil-Brown algae biodiesel Al_2O_3 and $C_{18}H_{34}O_2$,” *Elsev. Mater. Today Proceed.*, vol.33, pp.4192–4197, 2020.
- [16] S. Karthikeyan, A. Prathima, M. Periyasamy, and G. Mahendran, “Emission analysis of the diesel engine using *Stoechospermum marginatum*, brown marine algae with Al_2O_3 nano fluid,” *Elsev. Mater. Today Proceed.*, vol.33, pp.4047–4053, 2020.
- [17] S. Karthikeyan, A. Prathima, M. Periyasamy, and G. Mahendran, “Marine diesel engine using bio solar and gasoline,” *Elsev. Mater. Today Proceed.*, vol.33, pp.4132–4135, 2020.
- [18] S. Karthikeyan, A. Prathima, M. Periyasamy, and G. Mahendran, “Assessment of engine performance using syngas,” *Elsev. Mater. Today Proceed.*, vol.33, pp. 4142–4144, 2020.
- [19] S. Karthikeyan, A. Prathima, M. Periyasamy, and G. Mahendran, “Empirical studies upon the performance of the CI working with *Stoechospermum marginatum*, brown marine algae with nano fluid,” *Elsev. Mater. Today Proceed.*, vol.33, pp.3993–3999, 2020.
- [20] S. Karthikeyan, M. Periyasamy, A. Prathima and K. Sabariswaran, “Emission analysis of CI engine fueled with *S. Marginatum* macro algae biofuel – diesel blends,” *Elsev. Mater. Today Proceed.*, vol.33, pp.3458–3463, 2020.
- [21] S. Karthikeyan, M. Periyasamy, A. Prathima and K. Sabariswaran, “Performance analysis of diesel engine fueled with *S. marginatum* Macro algae biofuel - diesel blends,” *Elsev. Mater. Today Proceed.*, vol.33, pp.3464–3469, 2020.
- [22] S. Karthikeyan, M. Periyasamy, A. Prathima and K. Sabariswaran, “Combustion analysis of single-cylinder CI engine fueled with *S. Marginatum* Macro algae biofuel - diesel blends,” *Elsev. Mater. Today Proceed.*, vol.33, pp.3475–3480, 2020.
- [23] S. Karthikeyan, A. Prathima, and M. Periyasamy, “Characteristics studies on *Stoechospermum marginatum* brown marine algae with Al_2O_3 nanofluid,” *Elsev. Mater. Today Proceed.*, vol.33, pp.3746–3750, 2020.
- [24] S. Karthikeyan, A. Periyasamy, and A. Prathima, “Emission analysis of CI engine fueled by pilot dual fuel blends,” *Elsev. Mater. Today Proceed.*, vol.33, 3248–3253, 2020.
- [25] S. Karthikeyan, A. Prathima, M. Periyasamy, and G. Mahendran, “Emission analysis of the diesel engine using *Stoechospermum marginatum*, brown marine algae with Al_2O_3 nanofluid,” *Elsev. Mater. Today Proceed.*, vol.33, pp.4047–4053, 2020.
- [26] S. Karthikeyan, M. Periyasamy, and A. Prathima, “Biodiesel from microalgae Environmental aspects,” *Elsev. Mater. Today Proceed.*, vol.33, pp.3664–3667, 2020.
- [27] S. Karthikeyan, M. Periyasamy, A. Prathima, and M. Yuvaraja. M., “Agricultural tractor engine performance analysis using *Stoechospermum marginatum* microalgae biodiesel,” *Elsev. Mater. Today Proceed.* 33, pp.3438–3442, 2020.
- [28] S. Karthikeyan, M. Periyasamy, A. Prathima, and M. Ajai, “Effect of biosolar fuels and *S. Marginatum* algae biofuel on equivalence ratio in diesel engine with EGR,” *Elsev. Mater. Today Proceed.*, vol.33, pp.3443–3448, 2020.
- [29] S. Karthikeyan, M. Periyasamy, and A. Prathima, “Combustion analysis of CI engine using pilot dual fuel blends,” *Elsev. Mater. Today Proceed.*, vol.33, pp.3254–3259, 2020.
- [30] S. Karthikeyan, M. Periyasamy and A. Prathima, “Performance characteristics of CI engine using *Chlorella Vulgaris* microalgae oil as a pilot dual fuel blends,” *Elsev. Mater. Today Proceed.*, vol.33, pp.3277–3282, 2020.
- [31] S. Karthikeyan, M. Periyasamy, A. Prathima, and M. Ram Balaji, “Performance and exhaust emissions of a CI engine using Bi_2O_3 nano blends as an alternate

Caulerpa racemosa algae oil biofuel,” Elsev. Mater.
Today Proceed., vol. 33, pp.3265-3270, 2020.